Published as: *Nat Cell Biol*. 2013 July ; 15(7): 839–845.

A spindle-independent cleavage pathway controls germ cell formation in Drosophila

Ryan M. Cinalli[1] and **Ruth Lehmann**[1]

[1]HHMI and Kimmel Center for Biology and Medicine at the Skirball Institute, Department of Cell Biology, New York University School of Medicine, New York, NY 10016, USA

Abstract

The primordial germ cells (PGCs) are the first cells to form during *Drosophila melanogaster* embryogenesis. While the process of somatic cell formation has been studied in detail, the mechanics of PGC formation are poorly understood. Here, using 4D multi-photon imaging combined with genetic and pharmacological manipulations, we find that PGC formation requires an anaphase spindle-independent cleavage pathway. In addition to utilizing core regulators of cleavage, including the small GTPase RhoA (*Drosophila* Rho) and the Rho associated kinase, ROCK (*Drosophila* Rok), we show that this pathway requires Germ cell-less (Gcl), a conserved BTB-domain protein not previously implicated in cleavage mechanics. This alternate form of cell formation suggests that organisms have evolved multiple molecular strategies for regulating the cytoskeleton during cleavage.

Although insects of the order Diptera initially develop as large multinucleated cells, extensive cytoskeletal remodeling transforms the syncytial cell into a multicellular embryo by the start of gastrulation. This process of 'cellularization' has been best studied in *Drosophila melanogaster*[1-5]. Intriguingly, somatic cells and germ cell precursors (PGCs) require distinct genetic programs in order to cellularize. For example, somatic cell formation requires several zygotically transcribed gene products[6-12]. Together, these factors contribute to an essential feature of somatic cellularization: the synchronous ingression of newly synthesized membrane between, and then around individual nuclei[9]. In contrast, PGC formation is strictly controlled by maternal gene products collectively known as the germ plasm[13,14]. Since PGC formation has not been described in detail, the contribution of individual germ plasm components to this process is not understood and the defining feature(s) of this mode of cell formation remain unknown.

Several lines of evidence suggest that PGC formation may be similar to the process of animal cytokinesis[15]. For example, PGC formation, like cytokinesis, proceeds during

---

Correspondence should be addressed to R.L. ruth.lehmann@med.nyu.edu, Tel: 212 263 8071, Fax: 212 263 7760.

Author Contributions: R.M.C and R.L. conceived the project. R.M.C carried out the experiments and analyzed the data. R.M.C and R.L. wrote the paper.

Dedication: We dedicate this manuscript to the memory of Prof. Gerold Schubiger whose work in the early *Drosophila* embryo largely inspired the experiments presented here.

mitosis and requires the contractile ring components, Anillin and Diaphanous[16-18]. However, the strict dependence on germ plasm components for PGC formation suggests that cytokinesis alone is not sufficient to account for all aspects of this process. In particular, mutations in the germ plasm component, *gcl*, disrupt PGC formation but do not impact cytokinesis in other tissues[19].

To determine the mechanism of PGC formation, we began our studies by analyzing the events leading to PGC formation. When nuclei reach the embryonic cortex at the tenth nuclear cycle, they induce membrane and cytoplasmic protrusions, called 'buds'[4,20] (Supplementary Fig. S1a). Although the majority of these buds collapse shortly after their nuclei enter mitosis, the small fraction of buds that form within the germ plasm are reorganized into PGCs. To capture the transformation of buds into cells, we developed a 4D-imaging assay (Fig. 1a) that revealed and quantified the localization of green fluorescent protein (GFP), fused to either of two known cleavage furrow components, Myosin-II regulatory light chain-GFP (MRLC, *Drosophila* Sqh; now called 'Myosin-GFP') and Anillin-GFP (*Drosophila* Scraps), along with a kusabira orange fused germ plasm marker, Vasa-KO[21-23] (Fig. 1b and c). We found that both Anillin-GFP and Myosin-GFP were enriched at the neck of posterior buds (hereafter termed the 'bud furrow', BF)(Fig. 1d and e, Supplementary Fig. 1e). When nuclei within these buds entered mitosis, the BF constricted beneath the chromosomes, in a plane parallel to the mitotic spindle. During anaphase, a second cleavage furrow (hereafter termed the 'anaphase furrow', AF) assembled orthogonally to both the mitotic spindle and BF (Fig. 1b and c, Supplementary Fig. S1b and f, Supplementary Video S1 and S2). Although the AF ingressed asymmetrically, it divided the bud into two daughter cells in a manner similar to a cytokinetic furrow (Fig. 1c, Supplementary Fig. S1f). In contrast, BF cleavage separated the bud from the embryo, asymmetrically partitioning the germ plasm, marked by Vasa-KO, into the PGCs (Fig. 1c and Supplementary Video S2). Following their constriction, these paired furrows (AF-BF) resolved into a tripartite midbody-like structure that attached the newly formed cells to the embryonic cortex (Supplementary Fig. S1c and d). We conclude that the constriction of two orthogonally paired furrows remodels one bud into two PGCs (Fig. 1f).

What are the molecular mechanisms that control paired furrow activity during PGC formation? The small GTPase RhoA (*Drosophila* Rho) is a major regulator of cellular contractility and functions upstream of *anillin* and *diaphanous* during cytokinesis[24,25]. To determine whether PGC formation also requires RhoA activity, we injected the RhoA inhibitor, C3 peptide[26,27], into embryos shortly after bud formation. Injection of the C3 peptide, but not vehicle, blocked PGC formation (# embryos with PGCs, vehicle-injected = 15/15, C3-injected = 0/12) (Fig. 2a). In *Drosophila* S2 cells, RhoA targets Anillin to the cleavage furrow during cytokinesis[25]. Therefore, we asked whether targeting of Anillin-GFP to the BF was dependent on RhoA activity. Using our live imaging assay, we monitored Anillin-GFP at the BF following RhoA inhibition. In contrast to vehicle-controls, C3 peptide-injected embryos exhibited a 2.5-fold reduction in Anillin-GFP at the BF shortly after injection (Fig. 2b, Supplementary Video S3 and S4). These data demonstrate that PGC formation requires RhoA and suggest that a common RhoA signaling cascade regulates Anillin localization during both PGC formation and cytokinesis.

A major target of RhoA signaling during cytokinesis is the serine-threonine kinase, Rho-associated protein kinase (ROCK, *Drosophila* Rok). In *Drosophila*, ROCK promotes constriction of the cleavage furrow by phosphorylating serine and threonine residues in MRLC[28,29]. To ask whether ROCK acts downstream of RhoA during PGC formation, we injected embryos with a ROCK inhibitor, Y-27632, shortly after bud formation[30,31]. Injection of Y-27632, but not vehicle, blocked PGC formation in the majority of embryos assayed (# embryos with PGCs, vehicle-injected = 21/21, Y-27632-injected = 4/26) (Fig. 2c). Thus, we conclude that ROCK acts downstream of RhoA during PGC formation. Since MRLC is the major target of ROCK in *Drosophila*, these data suggest that myosin II activity is likely essential for both AF and BF cleavage.

During cytokinesis, the anaphase spindle signals to RhoA at the cell cortex to direct assembly and ingression of the cleavage furrow[32,33]. By coupling furrow assembly to the anaphase spindle, this mechanism ensures cleavage only after sister chromatid separation has begun. Because PGC formation, like cytokinesis, occurs during mitosis, we hypothesized that signaling from the anaphase spindle may activate RhoA to regulate paired furrow cleavage. To determine whether the anaphase spindle controls paired furrow assembly and/or constriction, we inhibited spindle assembly by injecting embryos with colcemid, which depolymerizes microtubules and arrests mitotic nuclei in metaphase. If paired furrow activity required anaphase spindle assembly, we reasoned that colcemid injection would prevent PGC formation. Surprisingly, we found that embryos injected with colcemid, but not vehicle, formed large, metaphase-arrested “PGC-like” cells (Fig. 2d) (# embryos with large, metaphase-arrested PGCs, vehicle-injected = 0/10, colcemid-injected = 16/18). To further investigate these findings, we injected embryos with colcemid and captured paired furrow behavior live using our 4D-imaging assay. Using Anillin-GFP to mark the furrows, we found that colcemid treatment blocked AF assembly in posterior buds, suggesting that the anaphase spindle may instruct AF assembly and constriction (Fig. 2e, Supplementary Fig. S2 and Supplementary Video 5). In contrast, BF constriction proceeded in colcemid-injected embryos, resulting in the formation of the large “PGC-like” cells (Fig. 2e, Supplementary Fig. S2 and Supplementary Video 5). Therefore, we conclude that BF cleavage is regulated in an anaphase spindle-independent manner. Moreover, these data illustrate that at least two distinct signaling pathways govern paired furrow activity.

What regulates anaphase spindle-independent BF cleavage during PGC formation? While syncytial nuclei reach the cortex of the embryo synchronously and form buds, only those nuclei surrounded by germ plasm become PGCs. Thus, we reasoned that components of the germ plasm likely played an instructive role in this mechanism of cellularization. Among known gene products localized to the germ plasm, *gcl* is an attractive candidate, since embryos that lack maternally deposited *gcl* (hereafter referred to as *gcl* mutant embryos) show specific defects in PGC formation[19,34]. The exact role of Gcl in this process, however, is unknown. We therefore analyzed AF and BF cleavage in *gcl* mutants using our live imaging assay. Mutant and control embryos exhibited an enrichment of Anillin-GFP at the BF, suggesting that Anillin is targeted to the BF independent of Gcl (Fig. 3a). However, despite AF assembly and cleavage, BF cleavage failed in mutant embryos, preventing PGC formation (Fig. 3a and Supplementary Video 6). We quantified the BF diameter shortly after

AF assembly in both control and mutant embryos and determined that mutants exhibited a 3-fold greater BF diameter (Fig. 3b). We conclude that BF, but not AF cleavage, requires Gcl and thus identify Gcl as the first unique regulator of spindle-independent cleavage.

Gcl is a BTB domain-containing protein that resides in the germ plasm and becomes enriched at the nuclear membrane of posterior buds prior to PGC formation[35]. Previous work suggested that Gcl represses transcription during PGC formation[34]. Our results suggest that Gcl may transcriptionally repress one or more negative regulators of BF cleavage. We tested this model by globally inhibiting Pol II dependent transcription, shortly after fertilization, by injecting α-amanitin and then assaying for PGC formation in control and *gcl* mutant embryos. We found that α-amanitin had no effect on PGC formation in control embryos (n = 15/15 embryos with > 15 pole cells), confirming that PGCs form in a transcription independent manner as reported previously[36]. Surprisingly, PGC formation was not rescued in α-amanitin-injected *gcl* embryos (n = 0/27 embryos with > 15 pole cells) (Supplementary Fig. S3). In these experiments, somatic cellularization was inhibited in all injected embryos, indicating that our injection assay efficiently inhibited Pol II-dependent transcription[3] (Supplementary Fig. S3). Thus, we conclude that Gcl does not inhibit Pol II dependent transcription during PGC formation.

We next considered whether Gcl counteracts the forces generated by the anaphase spindle during sister chromatid separation[37]. Our fixed tissue and live observations show that constriction of the BF coincides with the segregation of chromosomes towards opposing spindle poles (Supplementary Fig. S1f). Therefore, we hypothesized that Gcl may function to ‘stabilize’ the BF during this phase of mitosis. We reasoned that inhibiting assembly of the anaphase spindle might rescue BF cleavage in the *gcl* mutants. However, *gcl* mutants injected with colcemid, unlike controls, failed to form ‘PGC-like’ cells (# embryos with ‘PGC-like’ cells = 0/11) (Supplementary Fig S4, Supplementary Video 7 and 8). Therefore, we conclude that Gcl does not act to stabilize the BF during PGC formation.

Since Gcl overexpression within the germ plasm directs additional posterior buds to undergo PGC formation[38], we considered two final models, in which Gcl acts as either a permissive or instructive signal for BF cleavage. To distinguish between these two models, we filmed BF cleavage in control, *gcl* mutant and Gcl overexpressing (EP-*gcl*) embryos using our 4D-imaging assay (Supplementary Video 9, 10 and 11). We measured the BF diameter at several time points and calculated the rate of furrow constriction (Fig. 4a and b). If Gcl acts as a permissive cue, we would expect equal rates of constriction in control and Gcl overexpressing embryos. However, we found that the rate of constriction was proportional to the amount of Gcl present within the germ plasm (Fig. 4c). Indeed, even in control embryos, where the highest concentration of Gcl protein is found in the most posterior buds, we found a direct correlation between the position of the bud and the degree of BF constriction (Supplementary Fig. S5). Thus, we conclude that Gcl activity instructs BF cleavage by regulating the rate of furrow constriction.

While increased Gcl levels in the germ plasm result in supernumerary PGCs, mis-expression of *gcl* alone is not sufficient to cause ectopic cell formation[38]. However, ectopic expression of *gcl* at the anterior pole (*gcl-bcd*) causes defects in somatic cellularization[38]. To determine

how Gcl activity disrupts somatic cell formation, we immunostained control and Gcl mis-expressing embryos using an antibody against a somatic contractile ring component, Anillin. While constriction of the somatic contractile ring normally occurs only after membranes have surrounded the nuclei, we found that this Anillin-stained structure prematurely constricted in *gcl-bcd* embryos (Fig. 5a). Premature constriction of the contractile ring displaced somatic nuclei from the embryonic cortex and caused disruption of somatic cell organization. Thus, we conclude that Gcl is sufficient to promote constriction of the contractile ring independent of other germ plasm components. Because Gcl can influence the constriction behavior of both the BF and somatic contractile ring, we suggest that Gcl activity directly or indirectly regulates a core contractile component during cleavage.

Since Gcl and Anillin are both required for PGC formation[16,19] and because Gcl is not required for Anillin localization to the BF (Fig. 3a), we hypothesized that they may collaborate to promote BF cleavage. To test this model, we mis-expressed Gcl together with Anillin-GFP and scored ectopic cell formation at the anterior of the embryo. While neither protein alone was sufficient to direct BF cleavage of anterior buds, embryos mis-expressing both Gcl and Anillin-GFP induced some 'PGC-like' cells in several embryos (# of embryos scored with 'PGC-like' cells = 4/107)(Fig. 5b and e). While the extent of cell formation in these embryos did not approach the mis-expresssion of *oskar*[13] (# of embryos with Vasa positive cells =15/15) (Fig. 5b), we conclude that Gcl and Anillin represent the minimal molecular requirements for ectopic "PGC-like" cell formation during Drosophila embryogenesis.

In summary, we identify an alternate cleavage pathway that acts during the process of PGC formation and suggest that similar mechanisms may be utilized more broadly in biology. For example, the *Drosophila* neuroblast utilizes both spindle-dependent and -independent pathways to instruct cleavage during development[39]. Similar to *Drosophila* PGCs and neuroblasts, polar lobe formation in gastropods also appears to require spindle-independent cleavage[40,41]. In all three systems, the spindle-independent furrow partitions cytoplasmic determinants asymmetrically to instruct cell fates. One possibility is that these cleavage pathways initially co-evolved with mechanisms of cytoplasmic determination. In such a scenario, regulators of these alternative cleavage pathways, much like Gcl, are likely to reside within the determinate-rich cytoplasm of the differentiating daughter cell.

Gcl activity defines the only known molecular asymmetry between spindle-dependent and –independent cleavage pathways. While mammalian Gcl can act as a transcriptional regulator[42], our results reveal a transcription-independent role for *Drosophila* Gcl during BF cleavage. Regardless of its precise molecular function, mammalian Gcl has maintained an ability to instruct spindle-independent cleavage during the course of evolution as the mouse homolog can rescue PGC formation in *Drosophila* mutants[43]. In mammals, Gcl is required for spermatogenesis. Gcl mutant mice have defective sperm, with multi-nucleated heads and bent necks[44]. Reduced human *gcl* expression, along with defective sperm motility, has also been reported in azospermic men with normal karyotypes and intact Y-chromosomes[45]. Thus, Gcl may have a conserved role in regulating cytoskeletal or contractile behavior during germ line development in diverse animals.

Supplementary Material

Refer to Web version on PubMed Central for supplementary material.

Acknowledgments

We thank all members of the Lehmann lab for discussions and reagents. We thank Drs. Blum, Burden, Hurd, Slaidina, Teixeira and Zamparini for critical reading of the manuscript. We also thank Drs. Burden, Knaut, Nance, Schubiger, Small, Treisman and Wieschaus for discussions during the course of this work. This work was supported by a NSF Predoctoral Fellowship to R.M.C. R.L. is a Howard Hughes Medical Institute Investigator.

References

1. Sullivan W, Theurkauf WE. The cytoskeleton and morphogenesis of the early Drosophila embryo. Current opinion in cell biology. 1995; 7:18–22. [PubMed: 7755985]
2. Glover DM. Mitosis in the Drosophila embryo--in and out of control. Trends Genet. 1991; 7:125–132. [PubMed: 2068783]
3. Edgar BA, Kiehle CP, Schubiger G. Cell cycle control by the nucleo-cytoplasmic ratio in early Drosophila development. Cell. 1986; 44:365–372. [PubMed: 3080248]
4. Foe VE, Field CM, Odell GM. Microtubules and mitotic cycle phase modulate spatiotemporal distributions of F-actin and myosin II in Drosophila syncytial blastoderm embryos. Development. 2000; 127:1767–1787. [PubMed: 10751167]
5. Karr TL, Alberts BM. Organization of the cytoskeleton in early Drosophila embryos. The Journal of Cell Biology. 1986; 102:1494–1509. [PubMed: 3514634]
6. Wieschaus E, Sweeton D. Requirements for X-linked zygotic gene activity during cellularization of early Drosophila embryos. Development. 1988; 104:483–493. [PubMed: 3256473]
7. Simpson L, Wieschaus E. Zygotic Activity of the Nullo-Locus Is Required to Stabilize the Actin Myosin Network during Cellularization in Drosophila. Development. 1990; 110:851–863. [PubMed: 2088725]
8. Schejter ED, Wieschaus E. bottleneck acts as a regulator of the microfilament network governing cellularization of the Drosophila embryo. Cell. 1993; 75:373–385. [PubMed: 8402919]
9. Lecuit T, Wieschaus E. Polarized insertion of new membrane from a cytoplasmic reservoir during cleavage of the Drosophila embryo. The Journal of Cell Biology. 2000; 150:849–860. [PubMed: 10953008]
10. Lecuit T, Samanta R, Wieschaus E. slam encodes a developmental regulator of polarized membrane growth during cleavage of the Drosophila embryo. Developmental Cell. 2002; 2:425–436. [PubMed: 11970893]
11. Thomas JH, Wieschaus E. src64 and tec29 are required for microfilament contraction during Drosophila cellularization. Development. 2004; 131:863–871.10.1242/dev.00989 [PubMed: 14736750]
12. Stein JA, Broihier HT, Moore LA, Lehmann R. Slow as molasses is required for polarized membrane growth and germ cell migration in Drosophila. Development. 2002; 129:3925–3934. [PubMed: 12135929]
13. Ephrussi A, Lehmann R. Induction of germ cell formation by oskar. Nature. 1992; 358:387–392.10.1038/358387a0 [PubMed: 1641021]
14. Mahowald A. Assembly of the Drosophila germ plasm. Int Rev Cytol. 2001; 203:187–213. [PubMed: 11131516]
15. Green RA, Paluch E, Oegema K. Cytokinesis in animal cells. Annual review of cell and developmental biology. 2012; 28:29–58.10.1146/annurev-cellbio-101011-155718
16. Field CM, Coughlin M, Doberstein S, Marty T, Sullivan W. Characterization of anillin mutants reveals essential roles in septin localization and plasma membrane integrity. Development. 2005; 132:2849–2860.10.1242/dev.01843 [PubMed: 15930114]

17. Castrillon DH, Wasserman SA. Diaphanous is required for cytokinesis in Drosophila and shares domains of similarity with the products of the limb deformity gene. Development. 1994; 120:3367–3377. [PubMed: 7821209]
18. Afshar K, Stuart B, Wasserman SA. Functional analysis of the Drosophila diaphanous FH protein in early embryonic development. Development. 2000; 127:1887–1897. [PubMed: 10751177]
19. Jongens TA, Hay B, Jan LY, Jan YN. The germ cell-less gene product: a posteriorly localized component necessary for germ cell development in Drosophila. Cell. 1992; 70:569–584. [PubMed: 1380406]
20. Warn RM, Smith L, Warn A. Three distinct distributions of F-actin occur during the divisions of polar surface caps to produce pole cells in Drosophila embryos. The Journal of Cell Biology. 1985; 100:1010–1015. [PubMed: 3980576]
21. Karess RE, et al. The regulatory light chain of nonmuscle myosin is encoded by spaghetti-squash, a gene required for cytokinesis in Drosophila. Cell. 1991; 65:1177–1189. [PubMed: 1905980]
22. Field CM, Alberts BM. Anillin, a contractile ring protein that cycles from the nucleus to the cell cortex. The Journal of Cell Biology. 1995; 131:165–178. [PubMed: 7559773]
23. Hickson GRX, O'Farrell PH. Anillin: a pivotal organizer of the cytokinetic machinery. Biochem Soc Trans. 2008; 36:439–441.10.1042/BST0360439 [PubMed: 18481976]
24. Glotzer M. The molecular requirements for cytokinesis. Science. 2005; 307:1735–1739.10.1126/science.1096896 [PubMed: 15774750]
25. Hickson GRX, O'farrell PH. Rho-dependent control of anillin behavior during cytokinesis. Journal of Cell Biology. 2008; 180:285–294. [PubMed: 18209105]
26. Aktories K, Braun U, Rosener S, Just I, Hall A. The rho gene product expressed in E. coli is a substrate of botulinum ADP-ribosyltransferase C3. Biochemical and biophysical research communications. 1989; 158:209–213. [PubMed: 2492192]
27. Narumiya S, Sekine A, Fujiwara M. Substrate for botulinum ADP-ribosyltransferase, Gb, has an amino acid sequence homologous to a putative rho gene product. The Journal of biological chemistry. 1988; 263:17255–17257. [PubMed: 3141419]
28. Amano M, et al. Phosphorylation and activation of myosin by Rho-associated kinase (Rho-kinase). The Journal of biological chemistry. 1996; 271:20246–20249. [PubMed: 8702756]
29. Winter CG, et al. Drosophila Rho-associated kinase (Drok) links Frizzled-mediated planar cell polarity signaling to the actin cytoskeleton. Cell. 2001; 105:81–91. [PubMed: 11301004]
30. Narumiya S, Ishizaki T, Uehata M. Use and properties of ROCK-specific inhibitor Y-27632. Methods Enzymol. 2000; 325:273–284. [PubMed: 11036610]
31. Royou A, Sullivan W, Karess R. Cortical recruitment of nonmuscle myosin II in early syncytial Drosophila embryos: its role in nuclear axial expansion and its regulation by Cdc2 activity. The Journal of Cell Biology. 2002; 158:127–137.10.1083/jcb.200203148 [PubMed: 12105185]
32. Yuce O, Piekny A, Glotzer M. An ECT2-centralspindlin complex regulates the localization and function of RhoA. The Journal of Cell Biology. 2005; 170:571–582.10.1083/jcb.200501097 [PubMed: 16103226]
33. Su KC, Takaki T, Petronczki M. Targeting of the RhoGEF Ect2 to the Equatorial Membrane Controls Cleavage Furrow Formation during Cytokinesis. Developmental Cell. 2011; 21:1104–1115.10.1016/j.devcel.2011.11.003 [PubMed: 22172673]
34. Leatherman JL, Levin L, Boero J, Jongens TA. germ cell-less acts to repress transcription during the establishment of the Drosophila germ cell lineage. Curr Biol. 2002; 12:1681–1685. [PubMed: 12361572]
35. Jongens TA, Ackerman LD, Swedlow JR, Jan LY, Jan YN. Germ cell-less encodes a cell type-specific nuclear pore-associated protein and functions early in the germ-cell specification pathway of Drosophila. Genes & Development. 1994; 8:2123–2136. [PubMed: 7958883]
36. Lehner CF. The pebble gene is required for cytokinesis in Drosophila. Journal of cell science. 1992; 103(Pt 4):1021–1030. [PubMed: 1487486]
37. Civelekoglu-Scholey G, Scholey JM. Mitotic force generators and chromosome segregation. Cell Mol Life Sci. 2010; 67:2231–2250.10.1007/s00018-010-0326-6 [PubMed: 20221784]

38. Jongens T, Ackerman L, Swedlow J, Jan L, Jan Y. Germ cell-less encodes a cell type-specific nuclear pore-associated protein and functions early in the germ-cell specification pathway of Drosophila. Genes Dev. 1994; 8:2123–2136. [PubMed: 7958883]

39. Cabernard C, Prehoda KE, Doe CQ. A spindle-independent cleavage furrow positioning pathway. Nature. 2010; 467:91–94.10.1038/nature09334 [PubMed: 20811457]

40. Hejnol A, Pfannenstiel HD. Myosin and actin are necessary for polar lobe formation and resorption in Ilyanassa obsoleta embryos. Development Genes and Evolution. 1998; 208:229–233. [PubMed: 9634489]

41. Conrad GW, Schantz AR, Patron RR. Mechanisms of polar lobe formation in fertilized eggs of molluscs. Annals of the New York Academy of Sciences. 1990; 582:273–294. [PubMed: 2356981]

42. de la Luna S, Allen KE, Mason SL, La Thangue NB. Integration of a growth-suppressing BTB/POZ domain protein with the DP component of the E2F transcription factor. The EMBO journal. 1999; 18:212–228.10.1093/emboj/18.1.212 [PubMed: 9878064]

43. Leatherman JL, Kaestner KH, Jongens TA. Identification of a mouse germ cell-less homologue with conserved activity in Drosophila. Mechanisms of Development. 2000; 92:145–153. [PubMed: 10727854]

44. Kimura T, et al. Mouse germ cell-less as an essential component for nuclear integrity. Mol Cell Biol. 2003; 23:1304–1315. [PubMed: 12556490]

45. Kleiman SE, et al. Reduced human germ cell-less (HGCL) expression in azoospermic men with severe germinal cell impairment. J Androl. 2003; 24:670–675. [PubMed: 12954656]

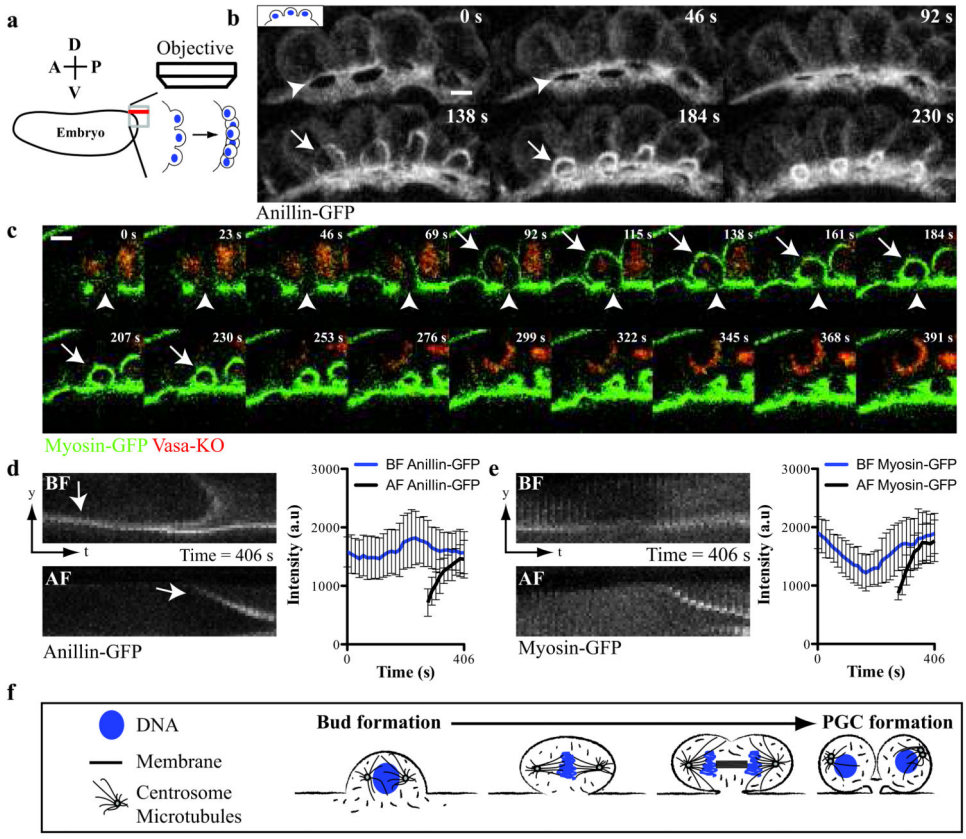

Figure 1. Anillin-GFP and Myosin-GFP localize to paired cleavage furrows during *Drosophila* PGC formation

(a) Diagram of 4D-imaging strategy used to capture PGC formation at the posterior of the *Drosophila* embryo. The embryo is positioned with its dorsal surface closest to the cover slip. 40 Z-slices (red line) spaced 1 μm apart along the dorsal-ventral axis were acquired per time point at the apex of the posterior pole. **(b)** Micrographs of time-lapse maximum intensity projections (MIP) of paired furrows during PGC formation revealed with Anillin-GFP (see Supplementary Video 1). **(c)** Time-lapse micrographs (single optical sections) of a single bud during PGC formation revealed by Myosin-GFP and Vasa-KO (see Supplementary Video 2). **(b, c)** Arrows and arrowheads mark the anaphase furrow (AF) and bud furrow (BF) respectively. **(d and e)** Kymographs showing the localization and quantification of **(d)** Anillin-GFP and **(e)** Myosin-GFP at a single paired furrow during PGC formation. We consistently observed biphasic enrichment of Myosin-GFP at the BF suggesting regulation by the cell cycle as previously reported[31]. Data shows the mean of quantifications done in **(d)** = 4 embryos and **(e)** = 4 embryos, with 3 buds measured in each embryo. Error bars: S.D. **(f)** Graphical description of PGC formation showing the remodeling of one bud into two cells. Scale bars = 5 μm

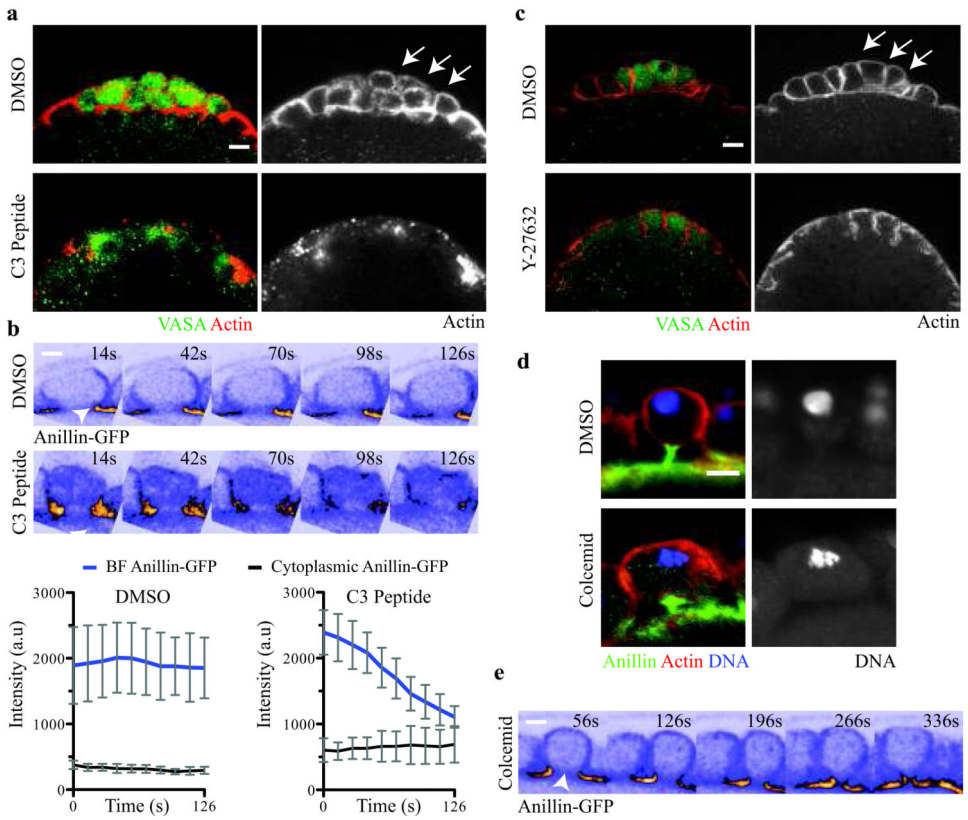

Figure 2. A spindle-independent cleavage pathway directs bud furrow cleavage

(a) Micrographs of vehicle- and C3 peptide-injected embryos (Vasa (green) and F-actin (red)). Arrows mark the PGCs in vehicle-injected embryos. Total number of embryos injected and scored in **(a)**: vehicle-injected = 15, C3 peptide-injected = 12. **(b)** Time–lapse micrographs and below quantification of Anillin-GFP at the BF in vehicle- and C3 peptide-injected embryos (see Supplementary Video 3 and 4). Arrowheads mark the BF. Quantification shows the mean of 4 embryos, with 3 buds measured in each embryo. Error bars: S.D. **(c)** Micrographs of vehicle- and Y27682-injected embryos (Vasa (green) and F-actin (red)). Arrows mark the PGCs in vehicle-injected embryos. Total number of embryos injected and scored in c: vehicle-injected = 21, Y27682-injected = 26. **(d)** MIP micrographs of single PGCs from vehicle- and colcemid-injected embryos (Anillin (green), F-actin (red) and DNA (blue)). Total number of embryos injected and scored in d: vehicle-injected = 10, colcemid-injected = 18. **(e)** Time-lapse micrographs (single optical sections) of a bud from a colcemid-injected Anillin-GFP expressing embryo showing complete constriction of BF (see Supplementary Video 5). Arrowhead marks the BF. Note the absence of the AF in the time series. Total number of embryos observed in e = 4. Scale bars = 5 μm

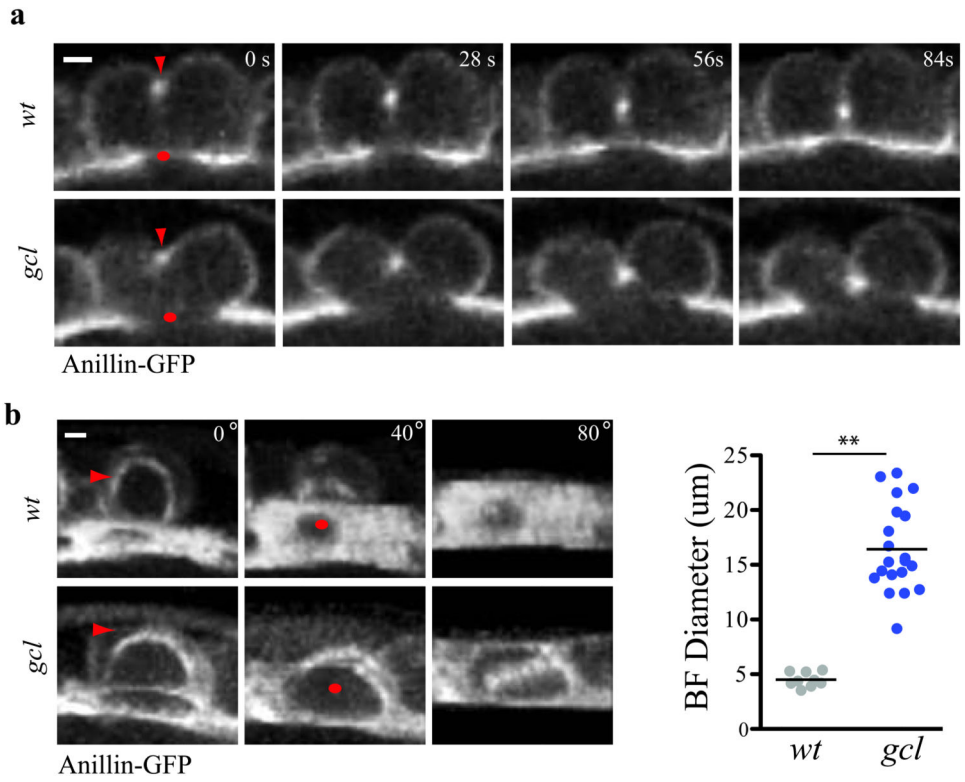

Figure 3. Germ cell-less is required for bud furrow constriction

(a) Time-lapse micrographs (single optical sections) of a single *wt* and *gcl* mutant bud during PGC formation revealed by Anillin-GFP. Red arrow marks the AF while a red dot marks the BF. Note BF constriction fails in the *gcl* mutant buds while AF forms and constricts. **(b)** MIP micrographs and quantification of the BF diameter shortly after AF formation in *wt* and *gcl* mutant buds. Red arrows mark the AF while red dots mark the BF. Each paired furrow is rotated around the X-axis by 40° and 80° to better reveal the BF. BF diameter was measured at t = AF formation in *wt* and *gcl* mutants. The total number of embryos filmed for b: *wt* = 4 and *gcl* = 7, where 1-3 BF diameters were measured per embryo. Total number of buds measured in b: *wt* = 9, *gcl* = 20. The black bar represents the mean BF diameter. ** represent a two-tailed t-test with $p < .001$.Scale bar = 5um.

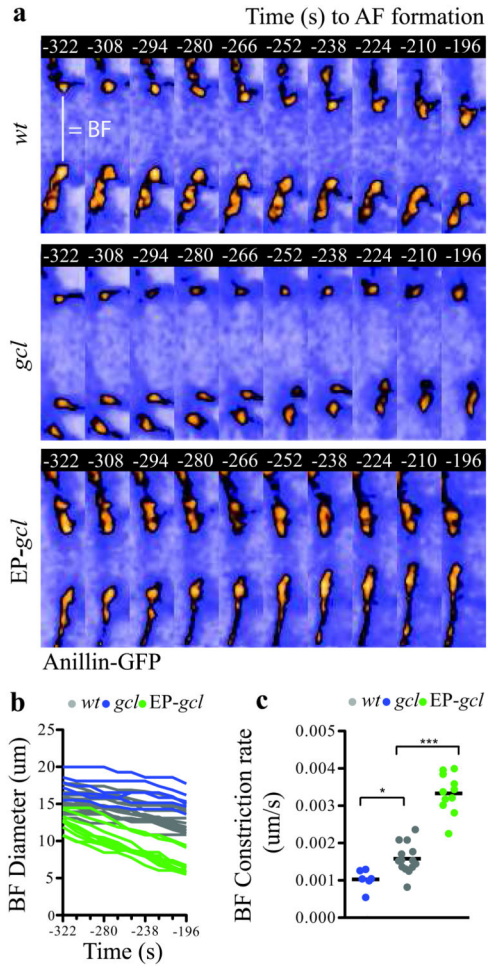

Figure 4. Germ cell-less is a rate-limiting component of bud furrow constriction

(a) Time-lapse micrographs (single optical sections) showing the BF diameter revealed with Anillin-GFP in *wt*, *gcl* mutant and Gcl-overexpressing embryos (EP-*gcl*) between t=-322s and t=-196s prior to AF formation (see Supplementary Video 6, 7 and 8). **(b)** Quantification of the BF diameter between t=-322s and t=-196s in *wt*, *gcl* mutant and EP-*gcl* embryos. **c**, BF rate of constriction between t=-322s and t=-196s in *wt*, *gcl* mutant and EP-*gcl* buds calculated from the slopes of the lines shown in **(b)**. Total number of embryos analyzed for c, d, e: *wt* = 7, *gcl* = 6, EP-*gcl* = 8, where 1 or 2 buds were measured in each embryo. One-way Anova: $p < .05$ for *wt* vs *gcl* and $p < .001$ for *wt* vs EP-*gcl*. Scale bars = 5 μm

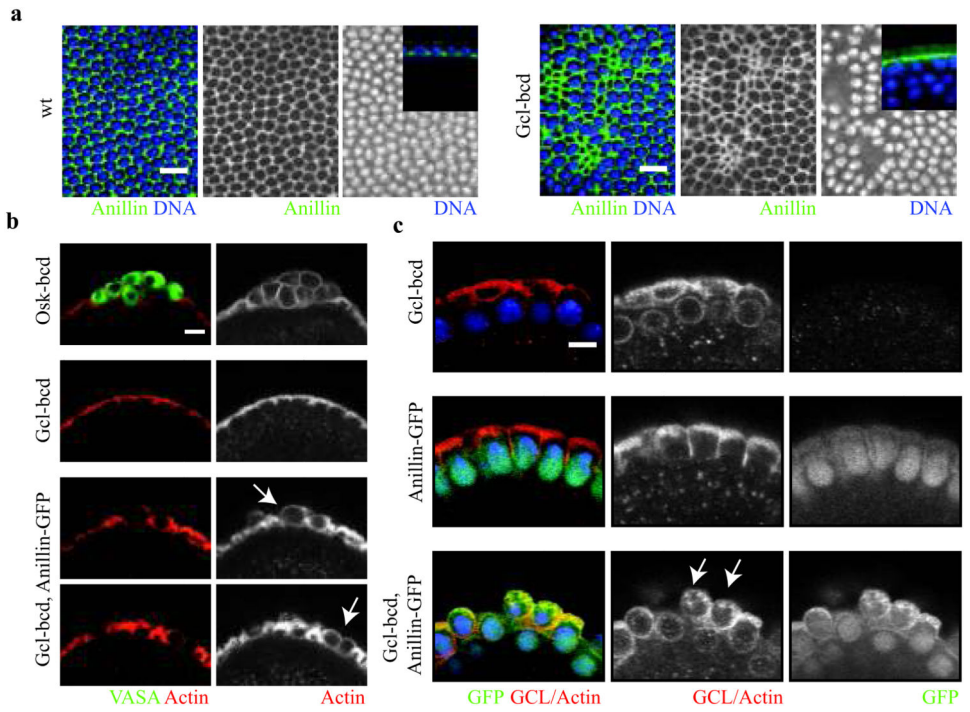

Figure 5. Mis-expression of Germ cell-less together with Anillin is sufficient for ectopic cell formation

(a) Surface micrographs of *wt* and Gcl mis-expressing embryos (*gcl-bcd*) during somatic cellularization (Anillin (green), and DNA (blue)). Note mis-expression disrupts somatic cell formation by inducing the premature constriction of the cellularization furrow. Insets are representative micrographs depicting lateral views of the cellularization furrow in *wt* and Gcl mis-expressing embryos.**(b)** Micrographs of the anterior pole of Oskar mis-expressing (*osk-bcd*), *gcl-bcd*, and *gcl-bcd, anillin-GFP* embryos (Vasa, germ plasm marker (green) and Actin (red)). Note Oskar is sufficient to ectopically recruit germ plasm (Vasa) and instruct cell formation, while *gcl-bcd, anillin-GFP* embryos instruct cell formation but do not recruit germ plasm. Arrows mark ectopic cells in *gcl-bcd, anillin-GFP* embryos prior to somatic cell formation. **(c)** Micrographs of the anterior pole of embryos from females expressing *gcl-bcd, anillin-GFP* and *gcl-bcd, anillin-GFP* transgenes (Anillin-GFP (green) GCL-Actin (red) and DNA (blue)). Arrows mark ectopic cells in *gcl-bcd, anillin-GFP* embryos at the start of somatic cell formation. Scale bars = 5 μm